Wind and Structures, Vol. 5, No. 2~4 (2002) 141-150
DOI: http://dx.doi.org/10.12989/was.2002.5.2_4.141

Numerical study of the effect of periodic jet excitation on cylinder aerodynamic instability

S. Hiejima†

Department of Environmental & Civil Engineering, Faculty of Environmental Science and Technology, Okayama University, 1-1, Tsushima-Naka, 3-chome, Okayama 700-8530, Japan

T. Nomura‡

Department of Civil Engineering, College of Science and Technology, Nihon University, 1-8-14, Kanda-Surugadai, Chiyoda-ku, Tokyo 101-8308, Japan

Abstract. Numerical simulations based on the ALE finite element method are carried out to examine the aerodynamics of an oscillating circular cylinder when the separated shear flows around the cylinder are stimulated by periodic jet excitation with a shear layer instability frequency. The excitation is applied to the flows from two points on the cylinder surface. The numerical results showed that the excitation with a shear layer instability frequency can reduce the negative damping and thereby stabilize the aerodynamics of the oscillating cylinder. The change of the lift phase seems important in stabilizing the cylinder aerodynamics. The change of lift phase is caused by the merger of the vortices induced by the periodic excitation with a shear layer instability frequency, and the vortex merging comes from the high growth rate, the rapid increase of wave number and decrease of phase velocity for the periodic excitation in the separated shear flows.

Key words: ALE; aerodynamic instability; circular cylinder; finite element method; periodic excitation; separated shear layer; shear layer instability; vortex-induced vibration.

1. Introduction

It is known that the vortex-induced vibration of an elastically supported body in a flow is caused by the interaction between the body motion and the unsteady separated shear flows around it. These flows are aerodynamically unstable and hence sensitive to the external disturbances such as acoustic excitation. Nishioka *et al*. (1990) reported that strong velocity fluctuations induced by acoustic excitation in the shear flow around an airfoil can suppress the flow separation from the airfoil surface. Similar acoustic excitation techniques have been applied to control the separated shear flow around an airfoil (Ahuja *et al*. 1983, Ahuja and Burrin 1984, Zaman *et al*. 1987, Hsiao *et al*. 1990, Zaman and McKinzie 1991, Zaman 1992) or to change the flow characteristics around a stationary circular cylinder (Peterka and Richardson 1969, Okamoto *et al*. 1981, Hsiao *et al*. 1989, Zobnin and Sushchik 1989, Hsiao and Shyu 1991, Sheridan *et al*. 1992). These studies show that

† Associate Professor
‡ Professor

the acoustic excitation with the shear layer instability frequency (f_{SL}) (Bloor 1964) is most effective in controlling the separated shear flows around a body. This type of excitation is mostly unstable and can therefore produce strong velocity fluctuations in the separated shear flows.

The previous experimental study conducted by the authors (Hiejima *et al*. 1995, 1996) has shown that stimulation of separated shear flows around a circular cylinder by acoustic excitation suppressed the vortex-induced vibration if the excitation has the frequency of f_{SL}, which was much higher than the Karman vortex-shedding frequency. In a previous numerical study (Hiejima *et al*. 1997), where the periodic jet excitation applied from a cylinder surface was employed for stimulating the shear flows, the excitation with f_{SL} is most effective in changing the surrounding flows due to its high growth rate in the shear flows. However, the suppression mechanism of the vortex-induced vibration by the periodic excitation with a frequency of f_{SL} is still not clarified.

The purpose of this study is to examine the effect of periodic jet excitation with f_{SL} on cylinder aerodynamic instability through numerical simulations. The suppression mechanism of vortex-induced vibration is also addressed. In order to simulate the incompressible viscous flow around an oscillating rigid cylinder, we employed a finite element method based on the arbitrary Lagrangian-Eulerian (ALE) formulation (Nomura *et al*. 1992, Nomura 1993, 1994).

2. Computational method

2.1. ALE description of the Navier-Stokes equations

The ALE formulation is based on a mixture of the classical Lagrangian and Eulerian descriptions. The motion of the mesh for the fluid analysis is prescribed corresponding to the cylinder motion. The Navier-Stokes equations based on ALE formulation with an incompressibility constraint are expressed as follows :

$$\rho\frac{\partial u_i}{\partial t} + \rho(u_j - \hat{u}_j)\frac{\partial u_i}{\partial x_j} = \frac{\partial \tau_{ij}}{\partial x_j} + f_i \tag{1}$$

$$\frac{\partial u_i}{\partial x_i} = 0 \tag{2}$$

where ρ is the density, u_i is the material velocity, $\hat{u}_i$ is the mesh velocity to describe mesh motion, τ_{ij} is the stress tensor, f_i is the body force. The convection velocity is replaced with the velocity $(u_i - \hat{u}_i)$ relative to the mesh velocity $\hat{u}_i$. The stress tensor τ_{ij} is given as

$$\tau_{ij} = -p\delta_{ij} + \mu\left(\frac{\partial u_i}{\partial x_j} + \frac{\partial u_j}{\partial x_i}\right) \tag{3}$$

where p is the pressure and μ is the coefficient of viscosity.

The finite element equations were obtained by applying the streamline upwind/Petrov-Galerkin method (Brooks *et al*. 1982) to the two-dimensional ALE Navier-Stokes equations with bilinear quadrilaterals for velocities and piecewise constants for pressure. In general, two-dimensional simulations of the flows around a body show slightly different results from three-dimensional simulations or wind tunnel experiments. However, the previous numerical study (Hiejima *et al*. 1997) has demonstrated that the two-dimensional simulation results agree qualitatively with the experimental results (Hiejima *et al*. 1995, 1996) for the effects of the periodic excitation on the flows around a circular cylinder and the vortex-induced vibration characteristics.

The finite element equations of motion and continuity are written as follows :

$$\boldsymbol{M}\boldsymbol{a} + \boldsymbol{N}(\boldsymbol{v} - \hat{\boldsymbol{v}})\boldsymbol{v} - \boldsymbol{G}\boldsymbol{p} = \boldsymbol{f} \tag{4}$$

$$\boldsymbol{G}^t\boldsymbol{v} = \boldsymbol{0} \tag{5}$$

where $\boldsymbol{M}$ and $\boldsymbol{G}$ are the mass and gradient matrices. $\boldsymbol{N}(\boldsymbol{v} - \hat{\boldsymbol{v}})$ accounts for convection and viscosity. $\boldsymbol{M}$, $\boldsymbol{N}$ and $\boldsymbol{G}$ are time dependent. $\boldsymbol{a}$, $\boldsymbol{v}$, $\hat{\boldsymbol{v}}$, $\boldsymbol{p}$ and $\boldsymbol{f}$ are the acceleration, material velocity, mesh velocity, pressure and force vectors, respectively.

2.2. Boundary conditions and finite element mesh

Fig. 1 shows the boundary conditions of the fluid domain, the material properties of the fluid and the parameters of the circular cylinder. The approaching flow velocity U is set at 26.4 cm/sec and the Reynolds number Re based on the cylinder diameter D is equal to 2000. A preliminary computation of the flow around the stationary cylinder has revealed that the Karman vortex-shedding frequency f_S is equal to 0.55 Hz, which corresponds to a Strouhal number of about 0.21 and agrees well with some other experimental results (Blevins 1990, Naudascher and Rockwell 1994).

Fig. 2 shows the finite element mesh. The ALE portion of the mesh is restricted to the square region around the cylinder, and the remaining part is left as Eulerian. The mesh velocities are equal to the cylinder velocity on the cylinder surface and zero on the external boundaries. They vary linearly in the region surrounded by the cylinder surface and the external boundaries. The number of

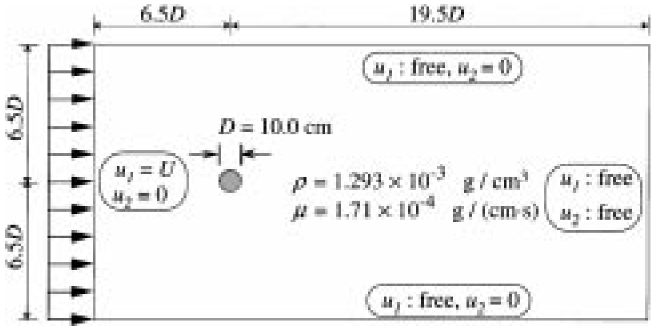

Fig. 1 Boundary conditions

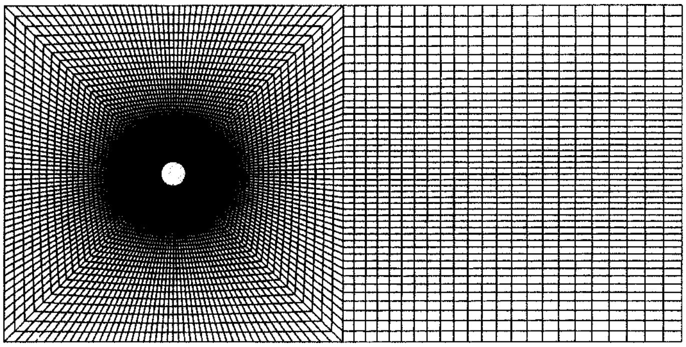

Fig. 2 Finite element mesh

finite element mesh cells used for the fluid domain is 13754, and the thickness of the mesh on the cylinder surface is 0.005*D*.

The predictor-corrector method (Brooks *et al*. 1982, Hughes 1987, Nomura *et al*. 1992) is employed for the time integration of the finite element equations, and the nondimensional time integration interval is set to 0.01.

2.3. Periodic jet excitation

The periodic jet excitation (Hiejima *et al.* 1997) for stimulating the separated shear flows is applied at two points of the cylinder surface, and then treated as a velocity boundary condition (Fig. 3). The angle ϕ_{ex} between the upstream stagnation point and the periodic excitation points is fixed at 80°, which is close to the separation point. The fluctuating velocity v_{ex} of the periodic excitation may be expressed as follows :

$$v_{ex} = U_{ex}\sin(2\pi f_{ex}t + \theta_{ex}) \tag{6}$$

where U_{ex}, f_{ex} and θ_{ex} represent the amplitude, the frequency and the phase of the periodic excitation, respectively. The excitation is defined as symmetric excitation when θ_{ex} are equal at the two excitation points, and as antisymmetric excitation when θ_{ex} at one excitation point is 180° prior to the other.

Bloor (1964) measured shear layer instability frequencies f_{SL} of the separated shear flows around a circular cylinder for various Reynolds numbers, and the regression curve of the experimental data is given as

$$\frac{f_{SL}}{f_S} = 0.1\sqrt{Re} \tag{7}$$

where f_S is Karman vortex-shedding frequency and Re is Reynolds number based on the cylinder diameter. Then $f_{SL} = 4.45\ f_S$ for $Re = 2000$, and f_{ex} was set at this shear layer instability frequency. The strength of the excitation was set at

$$C_q = \frac{q_{ex,rms}}{UD} = \frac{U_{ex}\Delta s}{\sqrt{2}\,UD} = 0.6(\%) \tag{8}$$

where $q_{ex,rms}$ indicates the r.m.s. value of the flux produced by the periodic excitation, and Δs is the length

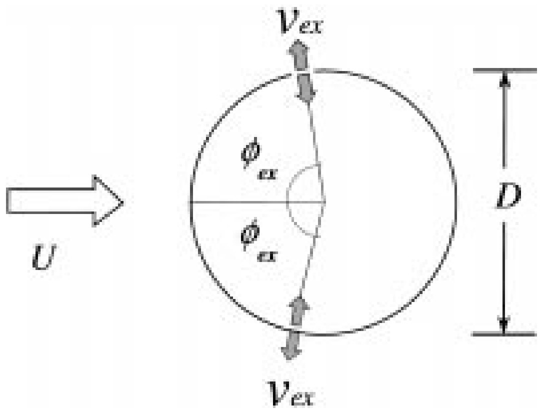

Fig. 3 Periodic jet excitation

of the mesh side where the periodic excitation is located. Although the analysis for the periodic excitation with $C_q = 1.2\%$ was also conducted, the results were qualitatively identical with those for $C_q = 0.6\%$.

2.4. Compatibility conditions between fluid variables and cylinder variables

Fluid variables on the cylinder surface must be constrained by cylinder variables such that :

$$\boldsymbol{a}^{\gamma} = \boldsymbol{T}^{t}\ddot{\boldsymbol{\delta}} \tag{9}$$

$$\boldsymbol{v}^{\gamma} = \boldsymbol{T}^{t}\dot{\boldsymbol{\delta}} \tag{10}$$

where $\boldsymbol{a}^{\gamma}$ and $\boldsymbol{v}^{\gamma}$ represent the acceleration and velocity of the fluid on the cylinder surface, respectively. $\ddot{\boldsymbol{\delta}}$ is the acceleratin vector of the cylinder. $\dot{\boldsymbol{\delta}}$ is the velocity vector of the cylinder. The transformation matrix $\boldsymbol{T}$ is derived from the geometrical relations between the center of gravity of the cylinder and the nodal coordinates of each node on the cylinder surface (Nomura *et al.* 1992).

For the specified two nodes where the periodic excitation is applied, the compatible conditions (9, 10) are replaced by

$$\boldsymbol{a}^{\gamma} = \boldsymbol{T}^{t}\ddot{\boldsymbol{\delta}} + \boldsymbol{a}^{ex} \tag{11}$$

$$\boldsymbol{v}^{\gamma} = \boldsymbol{T}^{t}\dot{\boldsymbol{\delta}} + \boldsymbol{v}^{ex} \tag{12}$$

where $\boldsymbol{a}^{ex}$ and $\boldsymbol{v}^{ex}$ are the acceleration and velocity vectors of the excitation, respectively.

3. Results and discussion

3.1. Effects on aerodynamic damping

In order to investigate the effect of the periodic jet excitation with a frequency of f_{SL} on unsteady lift force, we simulated the flow around an oscillating circular cylinder. The cylinder oscillation is prescribed in the across-flow direction. The amplitude z_0 of the cylinder displacement is kept at $0.2D$, and the nondimensional frequency $f_c^* = f_c\, D/U$ of the cylinder oscillation is varied from 0.19 to 0.28.

The unsteady lift force $L(t)$ of the oscillating cylinder is decomposed into $L_R(t)$ and $L_I(t)$, which are proportional to the cylinder displacement and the cylinder velocity, respectively. The lift coefficients of these components are obtained as

$$C_{LR} = \frac{2}{T}\int_0^T \frac{L(t)}{\frac{1}{2}\rho U^2 D}\,\frac{z_c(t)}{z_0}\,dt \tag{13}$$

$$C_{LI} = \frac{2}{T}\int_0^T \frac{L(t)}{\frac{1}{2}\rho U^2 D}\,\frac{\dot{z}_c(t)}{2\pi f_c z_0}\,dt \tag{14}$$

where $z_c(t)$ is the cylinder displacement and $\dot{z}_c(t)$ is the cylinder velocity.

Fig. 4 displays the component C_{LI} when no excitation, symmetric excitation or antisymmetric excitation is applied. When no excitation applied, over $f_c^* = 0.19$~0.23, C_{LI} has a positive value. This means the cylinder has a negative damping and is therefore aerodynamically unstable.

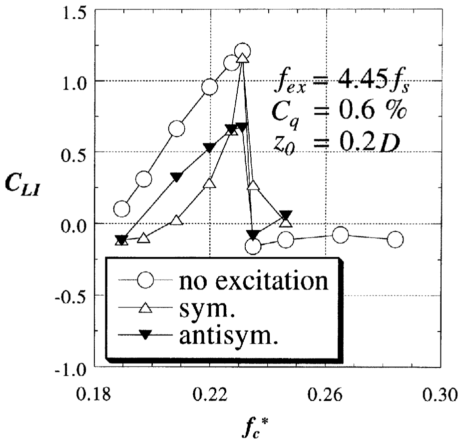

Fig. 4 Lift coefficient proportional to cylinder velocity

When the symmetric or antisymmetric excitation is applied, due to the reduction of C_{LI} over this cylinder frequency range, the cylinder becomes more stable than the case of no excitation.

In order to investigate the main cause of the reduction of C_{LI} due to the periodic excitation, we analyzed the lift phase lag β_L relative to the cylinder displacement and the absolute value $|C_L|$ of the lift coefficient. These parameters are obtained by

$$\beta_L = \tan^{-1}(C_{LI}/C_{LR}) \tag{15}$$

$$|C_L| = \sqrt{C_{LR}^2 + C_{LI}^2} \tag{16}$$

and then C_{LI} can be expressed as

$$C_{LI} = |C_L| \sin\beta_L \tag{17}$$

Over $f_c^* = 0.19$~0.23, where C_{LI} was reduced by the periodic excitation, for both symmetric and antisymmetric excitation β_L is higher and moves further from 90° than the case of no excitation (see Figs. 4 and 5). According to Eq. (17), this phase precedence of lift has a reducing effect on C_{LI}, and is consistent with the reduction of C_{LI} in Fig. 4. However, $|C_L|$ is not necessarily reduced by the periodic excitation in the same cylinder frequency range (Fig. 6) and hence not consistent with the result in Fig. 4. Consequently, these results tell us that the reduction of C_{LI} probably results from a change of β_L rather than a reduction of $|C_L|$.

The time histories of the unsteady lift for $f_c^* = 0.21$ demonstrate also the phase precedence of lift due to the excitation (Fig. 7). Moreover, this figure tells us that the phase precedence of lift occurs intermittently. This intermittency of the lift phase precedence was also observed at some other cylinder frequencies.

3.2. Change of flows around the cylinder

Fig. 8 presents the instantaneous vorticity contours at the same phase of cylinder oscillation with $f_c^* = 0.21$. The shear flows just behind the cylinder oscillate in the across-flow direction and just move downward in these figures. When the symmetric or the antisymmetric excitation is applied, the shear flows are inclined downward compared to those of no excitation. This means the phases of

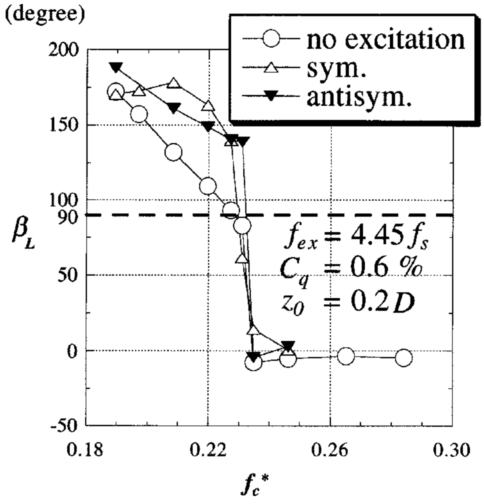

Fig. 5 Phase lag of unsteady lift

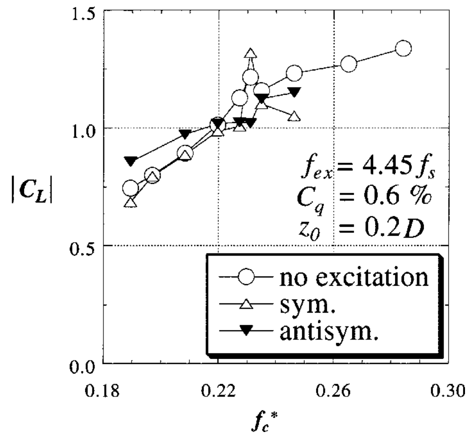

Fig. 6 Absolute value of unsteady lift

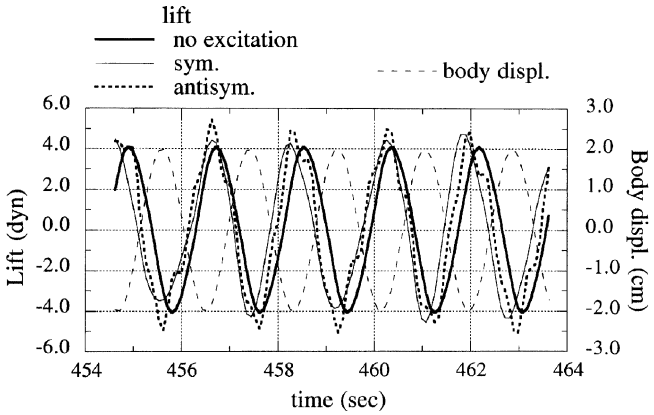

Fig. 7 Phase precedence of lift by periodic excitation

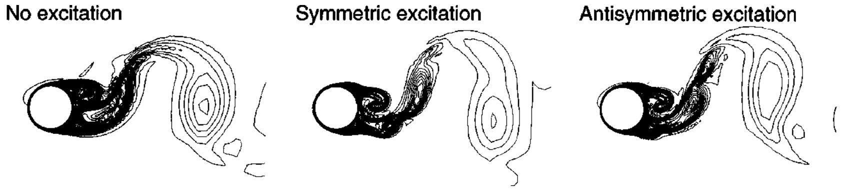

Fig. 8 Phase precedence of shear flow oscillation by periodic excitation

shear flow oscillation for the symmetric and antisymmetric excitation are prior to the phase for no excitation, which leads to the phase precedence of lift. It is also found that strength of the shear flow oscillation behind the cylinder was not changed significantly by the periodic excitation. These results about the phase and the strength of shear flow oscillation qualitatively agree with Figs. 5 and 6.

Fig. 9 shows the behaviour of the vortices induced by the symmetric and antisymmetric excitation in the separated shear flows. As shown in a series of figures, two vortices induced by the excitation

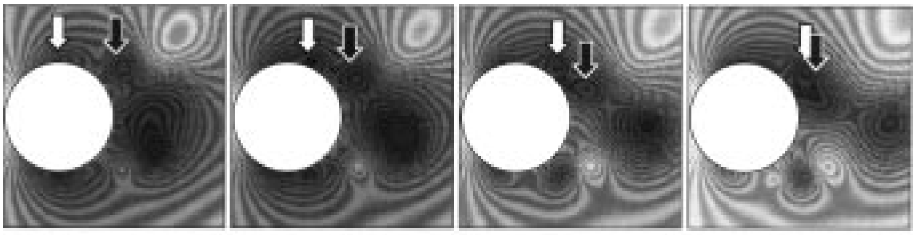

(a) Symmetric excitation

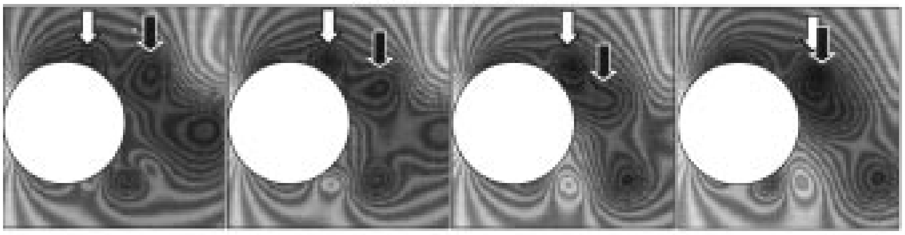

(b) Antisymmetric excitation

Fig. 9 Merger of the vortices induced by periodic excitation in the shear flow

merge and become a larger vortex in the upper shear flow. Such vortex merging was found to occur frequently and affect the heaving motion of the shear flow oscillation. Accordingly, these vortices seem to cause the phase precedence of shear flow oscillation.

3.3. Relation to shear layer instability

The vortices induced by the periodic excitation come from the enhancement of fluctuation by the shear layer instability. The shear layer instability can be theoretically evaluated by applying the linear stability analysis (Gaster 1965, Michalke 1965, Nishioka *et al*. 1990) to the mean velocity distribution of the shear flow around a body. The stability calculation is made on the basis of Rayleigh equation by assuming parallel flow.

The mean velocity distributions of the shear flows near the cylinder surface are selected as the basic flow for the stability calculation (Fig. 10). These distributions were obtained from the previous numerical simulation (Hiejima *et al*. 1997) at the angle $\theta = 61^o \sim 94^o$ from the down-stream stagnation point. The calculation made is of the spatially growing type, and the results for the Bloor's shear layer instability frequency of 4.45 f_S are shown in Fig. 11, compared to the frequency of f_S. In these figures, $-\alpha_i$ and α_r are the eigenvalues (growth rate and wave number), and $c_r (=2\pi f/\alpha_r)$ is the phase velocity, respectively.

Fig. 11(a) confirms the high growth rate for 4.45 f_S in the separated shear flows around the cylinder. Then the periodic excitation with the Bloor's shear layer instability frequency is enhanced due to its high growth rate and generates discrete vortices in the shear flows. Furthermore, the rapid increase of wave number and decrease of phase velocity for 4.45 f_S near $60^o \sim 70^o$ in Figs. 11(b)(c) confirm the decrease of the distance between the vortices with the frequency of 4.45 f_S and the decrease of the convection velocity of these vortices. Accordingly, these results imply the frequent occurrence of the merger of the discrete vortices induced by the periodic excitation with the Bloor's shear layer instability frequency behind the cylinder (see Fig. 9).

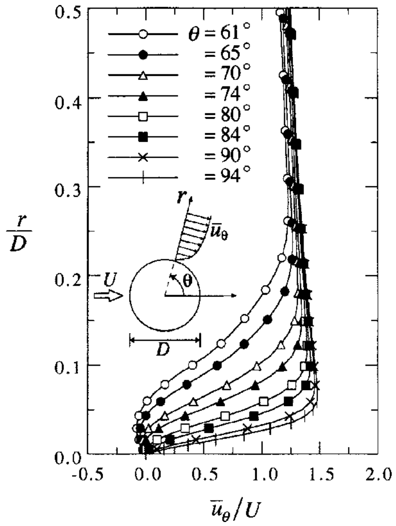

Fig. 10 Mean velocity distributions near the cylinder surface

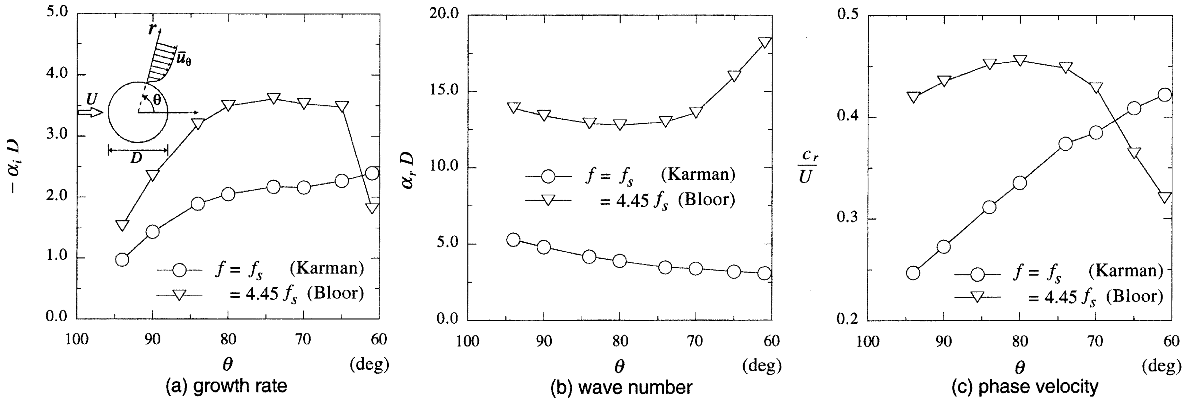

Fig. 11 Shear layer instability for the Bloor's frequency

4. Conclusions

The effect of periodic jet excitation with a shear layer instability frequency on cylinder aerodynamic instability has been examined by using the ALE finite element method. The periodic excitation, which was applied from the cylinder surface, stimulated the separated shear flows around the cylinder. The numerical results showed that the periodic excitation with a shear layer instability frequency can reduce the negative damping and thereby stabilize the aerodynamics of the oscillating cylinder. The change of the lift phase, which is caused by the merger of the vortices induced by the periodic excitation, seems important in stabilizing the cylinder aerodynamics and then suppressing the vortex-induced vibration. The linear stability analysis indicated the high growth rate, the rapid increase of wave number and decrease of phase velocity for the fluctuation with the shear layer instability frequency in the separated shear flows. This instability generates discrete vortices by applying the periodic excitation with the shear layer instability frequency and causes the merger of these vortices frequently, thereby changing the lift phase.

Acknowledgements

This work was supported partly by The Sumitomo Foundation and The Yakumo Foundation for Environmental Science. We would like to acknowledge the generosity of these organizations.

References

Ahuja, K.K., et al. (1983), "Control of turbulent boundary layer flows by sound", *AIAA Paper*, 83-0726.

Ahuja, K.K. and Burrin, R.H. (1984), "Control of flow by sound", *AIAA Paper*, 84-2298.

Blevins, R.D. (1990), *Flow-Induced Vibration, Van Nostrand Reinhold*, New York.

Bloor, M.S. (1964), "The transition to turbulence in the wake of a circular cylinder", *J. Fluid Mech.*, **19**, 290-304.

Brooks, A.N., et al. (1982), "Streamline upwind/Petrov-Galerkin formulations for convection dominated flows with particular emphasis on the incompressible Navier-Stokes equation", *Comput. Meths. Appl. Mech. Engrg.*, **32**, 199-259.

Gaster, M. (1965), "On the generation of spatially growing waves in a boundary layer", *J. Fluid Mech.*, **22**, 433-441.

Hiejima, S. et al., (1995), "An experimental study on the effect of applied sound on the vortex-induced vibration of a circular cylinder", *Proc. EASEC-5*, 1231-1236.

Hiejima, S. et al., (1996), "An experimental study on the control of the vortex-induced vibration of a circular cylinder by acoustic excitation", *Struct. Eng./Earthquake Eng. (JSCE)*, **13**(1), 67s-72s.

Hiejima, S. et al., (1997), "Numerical study on the suppression of the vortex-induced vibration of a circular cylinder by acoustic excitation", *J. Wind Eng. Ind. Aerod.*, **67 & 68**, 325-335.

Hsiao, F.B. et al., (1989), "Experimental study of an acoustically excited flow over a circular cylinder", *Transport Phenomena in Thermal Control* (ed. G. J. Hwang), New Youk : Hemisphere, 537-546.

Hsiao, F.B. et al., (1990), "Control of wall-separated flow by internal acoustic excitation", *AIAA Journal*, **28**, 1440-1446.

Hsiao, F.B. and Shyu, J.Y. (1991), "Influence of internal acoustic excitation upon flow passing a circular cylinder", *J. Fluids Struct.*, **5**, 427-442.

Hughes, T.J.R. (1987), *The Finite Element Method*, Prentice-Hall, New Jersey.

Michalke, A. (1965), "On spatially growing disturbances in an inviscid shear layer", *J. Fluid Mech.*, **23**, 521-544.

Naudascher, E. and Rockwell, D. (1994), *Flow-Induced Vibrations*, A. A. Balkema, Rotterdam, Netherlands.

Nishioka, M. et al., (1990), "Control of flow separation by acoustic excitation", *AIAA Journal*, **28**(11), 1909-1915.

Nomura, T. et al., (1992), "An arbitrary Lagrangian-Eulerian finite element method for interaction of fluid and a rigid body", *Comput. Meths. Appl. Mech. Engrg.*, **95**, 115-138.

Nomura, T. (1993), "Finite element analysis of vortex-induced vibrations of bluff cylinder", *J. Wind Eng. Ind. Aerod.*, **46 & 47**, 587-594.

Nomura, T. (1994), "ALE finite element computations of fluid-structure interaction problems", *Comput. Meths. Appl. Mech. Eng.*, **112**, 291-308.

Okamoto, S. et al. (1981), "The effect of sound on the vortex-shedding from a circular cylinder", *Bull. JSME*, **24**(187), 45-53.

Peterka, J.A. and Richardson, P.D. (1969), "Effect of sound on separated flows", *J. Fluid Mesh.*, **37**(2), 265-287.

Sheridan, J. et al. (1992), "The Kelvin-Helmholtz instability of the separated shear layer from a circular cylinder", *Proc. IUTAM Symp. on Bluff-Body Wakes, Dynamics and Instabilities* (ed. H. Eckelmann *et al.*), Berlin : Springer-Verlag, 115-118.

Zaman, K. B. M. Q. et al. (1987), "Effect of acoustic excitation on the flow over a low-Re air-foil", *J. Fluid Mech.*, **182**, 127-148.

Zaman, K. B. M. Q. and McKinzie, D.J. (1991), "Control of laminar separation over airfoils by acoustic excitation", *AIAA Journal*, **29**, 1075-1083.

Zaman, K. B. M. Q. (1992), "Effect of acoustic excitation on stalled flows over an airfoil", *AIAA Journal*, **30**, 1492-1499.

Zobnin, A.B. and Sushchik, M.M. (1989), "Influence of a high-frequency sound field on vortex-generation in the wake of a cylinder", *Sov. Phys. Acoust.*, **35**(1), 37-39.